3.3 Strongly Correlated Quantum Systems

Numerical analysis for extotic quantum states in strongly correlated electron systems

Akihisa Koga
Department of Physics, Tokyo Institute of Technology, Meguro, Tokyo 152-8551

Strongly correlated electron systems with orbital degrees of freedom have attracted much interest. One of the intriguing examples is the series of the Mott insulators with a honeycomb structure such as A_2IrO_3 ($A = Na, Li$), and β-Li_2IrO_3. In these compounds, a strong spin-orbit coupling for $5d$ electrons lifts the degeneracy in t_{2g} levels and the Kramers doublet plays an important role at low temperatures. Furthermore, there exists the orbital dependent hoppings due to the lattice structure. These result in the anisotropy in the exchange coupling between isospins, and the system can be regarded as the $s = 1/2$ Kitaev model [1, 2]. This should stimulate the extensive theoretical study for the Kitaev and related models. Recently, the compound α-$RuCl_3$ with $4d$ electrons has been synthesized and fermionic response characteristic of the Kitaev model has been discussed. In general, in the $4d$ electron system, the spin-orbit coupling is not so large, comparing with the $5d$ electron system. Therefore, a simple question naturally arises how the finite spin-orbit interaction realizes interesting ground-state and low temperature properties. Furthermore, the above compounds show the magnetic order at low temperatures, and it is desired to clarify the stability of the spin liquid state in the correlated electron system with the orbital degeneracy.

Motivated by this, we have studied the spin-orbital models with the Kugel-Khomskii type superexchange interactions on the two-dimensional honeycomb lattice. Since this model is reduced to the Kitaev model in the large spin-orbit coupling limit (Kitaev limit), we can discuss how the disordered state, which is adiabatically connected to the spin liquid state in the Kitaev limit, competes with the magnetically ordered state naively expected. We first use the cluster mean-field theory with the exact diagonalization to determine the ground state phase diagram in the model (see Fig. 1). Furthermore, calculating the specific heat and entropy in terms of the thermal pure quantum state, we have discussed how thermodynamic properties characteristic of the Kitaev model appear in the intermediate spin-orbit coupling region [3].

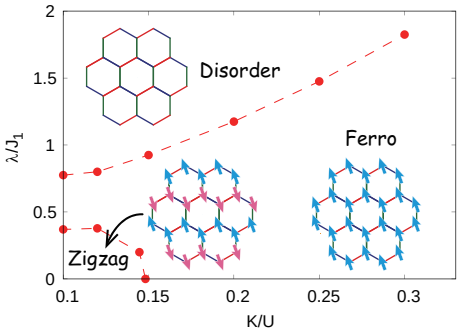

Figure 1: The ground state phase diagram of the spin-orbital model.

[C class 7000 (B); D class; 8000 (B)]

References

[1] A. Kitaev, Ann. Phys. **321**, 2 (2006).

[2] G. Jackeli and G. Khaliullin, Phys. Rev. Lett. **102**, 017205 (2009).

[3] A. Koga, S. Nakauchi, and J. Nasu, Phys. Rev. B **97**, 094427 (2018).

Study of correlated topological materials using many-variable variational Monte Carlo method

Takahiro Misawa
Institute for Solid State Physics, University of Tokyo
Kashiwa-no-ha, Kashiwa, Chiba 277-8581

Topological insulators that show exotic surface metallic states [1] have been attracted much attention because the topologically protected metallic surface states are expected to be useful for new generation devices. Recent theoretical and experimental studies have proven the existence of the topological *semimetals* [2] such as the Weyl semimetals and the topological Dirac semimetal. In these topological semimetals, although the bulk gap is zero and the point nodes such as the Weyl points or the Dirac points exist in the bulk state, the exotic surface states called Fermi arcs appear.

In this project, we study the quantum transport phenomena originating the exotic surface states in the topological semimetals by directly solving the time-dependent Schrödinger equations, which is given by

$$\mathrm{i}\frac{\partial\left|\phi(t)\right\rangle}{\partial t} = H(t)\left|\phi(t)\right\rangle, \tag{1}$$

where $|\phi(t)\rangle$ is a single Slater determinant and $H(t)$ is time-dependent Hamiltonian. To efficiently solve the time-dependent Schrödinger equations, we use the fourth-order Suzuki-Trotter decomposition [3, 4].

We first analyze the charge pumping in the disordered Weyl semimetal. To perform the charge pumping we introduce the time-dependent vector potentials $A_y(t)$ in y direction as follows:

$$T_y(t) = e^{\mathrm{i}A_y(t)} \times T_y, \tag{2}$$

$$A_y(t) = \frac{2\pi t}{L_y T}, \tag{3}$$

where T_y is the hopping matrix in y direction and L_y is the linear dimension in y direction. By introducing $A_y(t)$ in y direction, the charge pumping in x directions occurs if the Hall conductivity is finite. Actually in the clean limit, we confirm that the charge pumping ΔN is quantized [5, 6, 7] as follows:

$$\Delta N = 2\Delta k \times \frac{L_z}{2\pi}, \tag{4}$$

where L_z is the linear dimension in z direction and Δk is the distance between Weyl points in the momentum space. We examine the effects of the disorders in the chemical potentials and show that charge pumping is robust against the disorders. Interestingly, the charge pumping is enhanced in the intermediate strength of the disorder, which is consistent with previous studies [8, 9, 10].

By using the same method, we analyze the quantum transport phenomena in the bilayer system of the ferromagnetic insulator and the topological Dirac semimetals. In this system, we show that the oscillating magnetic moment in the ferromagnetic insulator induces the spin and charge current in the topological Dirac semimetals. We also show that the induced charge current is governed by the topological nature and robust against the disorder.

These results show that real-time evolution of the wave functions is useful for analyzing the exotic quantum transport phenomena in the topological materials. The real-time evolution of the correlated quantum many-body system is possible based on the variation Monte Carlo

method [11, 12]. By using the many-variable variational Monte Carlo method [13, 14], we are now examining the stability of the topological magnetic insulators (Chern insulator) in the correlated electron systems. We are also examining the quantum transport phenomena in the topological magnetic insulators by using the real-time evolution of the correlated many-body wavefunctions.

References

[1] M. Z. Hasan, C. L. Kane, Rev. Mod. Phys. **82**, 3045 (2010).

[2] A. Burkov, Nat. Mat. **15**, 1145 (2016).

[3] M. Suzuki, Commun. Math. Phys. **163**, 491 (1994).

[4] T. Nakanishi, T. Ohtsuki, T. Kawarabayashi, J. Phys. Soc. Jpn. **66**, 949 (1997).

[5] R. Shindou, N. Nagaosa, Phys. Rev. Lett. **87**, 116801 (2001).

[6] S. Murakami, New Journal of Physics **9**, 356 (2007).

[7] X. Wan, A. M. Turner, A. Vishwanath, S. Y. Savrasov, Phys. Rev. B **83**, 205101 (2011).

[8] C.-Z. Chen, J. Song, H. Jiang, Q.-f. Sun, Z. Wang, X. C. Xie, Phys. Rev. Lett. **115**, 246603 (2015).

[9] H. Shapourian, T. L. Hughes, Phys. Rev. B **93**, 075108 (2016).

[10] Y. Takane, J. Phys. Soc. Jpn. **85**, 124711 (2016).

[11] G. Carleo, F. Becca, M. Schiró, M. Fabrizio, Sci. Rep. **2**, 243 (2012).

[12] K. Ido, T. Ohgoe, M. Imada, Phys. Rev. B **92**, 245106 (2015).

[13] D. Tahara, M. Imada, J. Phys. Soc. Jpn. **77**, 114701 (2008).

[14] T. Misawa, S. Morita, K. Yoshimi, M. Kawamura, Y. Motoyama, K. Ido, T. Ohgoe, M. Imada, T. Kato, arXiv:1711.11418.

Numerical study of correlated electron systems with strong spin-orbit coupling

Yukitoshi MOTOME

Department of Applied Physics,

The University of Tokyo, Bunkyo, Tokyo 113-8656

We have theoretically studied intriguing properties originating from electron correlations and spin-orbit coupling. During this fiscal year (project number: H29-Ca-0060 and H29-Cb-0034), we have been making substantial progress on the following topics. We summarize the main achievements for each topic below.

(i) *Exotic magnetism and electronic states in spin-charge coupled systems*: We constructed a new effective spin model for the Kondo lattice model, on the basis of higher-order perturbation theory in terms of the spin-charge coupling [1]. The model includes the bilinear and biquadratic spin interactions in momentum space: the exchange interactions are characterized by specific wave numbers dictated by the Fermi surfaces. We demonstrated that the model well reproduces variety of peculiar magnetic orders, such as vortex crystals and skyrmion crystals. We also extended the study to the systems with the relativistic spin-orbit coupling and predicted the realization of unconventional skyrmions [2]. Another topic is the chiral soliton lattice in quasi-one-dimensional chiral magnets. To clarify the magnetic and electronic properties, we have studied a model explicitly including itinerant electrons. By Monte Carlo simulations at finite temperature, we revealed nonlinear magnetoresistance proportional to the soliton density [3]. We also found lock-in of the period of chiral soliton lattices at a particular set of values related with the Fermi wave number [4]. In addition, we studied the generation and control of exotic magnetism by supercurrent in heterostructures [5].

(ii) *Off-diagonal and nonreciprocal responses in parity broken systems*: We analyzed a model for e_g electron systems on a diamond structure, bearing $A\mathrm{OsO_4}$ (A=K, Rb, and Cs) in mind [6]. We predicted possible band structures and magnetoelectric responses under various electronic orders that break spatial inversion symmetry. The results will be useful for identifying the unknown order parameters in $A\mathrm{OsO_4}$. We also summarized the first-principles studies for honeycomb-monolayer transition metal trichalcogenides [7]. In addition, we studied bilayer and bulk cases [8]. Furthermore, we investigated the nonreciprocal spin Seebeck effect in antiferromagnets with asymmetric magnon dispersions [9]. We

theoretically predicted spin rectification and directional dependence of the nonreciprocal spin Seebeck effect.

(iii) *Spin fractionalization in the Kitaev models*: We summarized our studies on spin dynamics at finite temperature in the Kitaev models, obtained by the newly-developed numerical techniques on the basis of Majorana fermion representation [10,11]. Comparing our results with those by inelastic neutron scattering for a candidate material α-$RuCl_3$, we found a good agreement in a wide range of energy scale and temperature [12]. We also studied thermal conductivities in the Kitaev model [13] and compared the results with experiments [14]. In addition, we studied a gas-liquid type phase transition on a hyperoctagon lattice [15], and phase transitions to chiral spin liquids on a hypernonagon lattice [16]. We also proposed a new mechanism for the Kitaev type anisotropic interactions in d^7 high-spin systems [17].

References

[1] S. Hayami, R. Ozawa, and Y. Motome, Phys. Rev. B **95** (2017) 224424. [*selected in Kaleidoscope*]

[2] S. Hayami and Y. Motome, preprint (arXiv:1803.01543).

[3] S. Okumura, Y. Kato, and Y. Motome, J. Phys. Soc. Jpn. **86** (2017) 063701.

[4] S. Okumura, Y. Kato, and Y. Motome, J. Phys. Soc. Jpn. **87** (2018) 033708.

[5] R. Takashima, Y. Kato, Y. Yanase, and Y. Motome, Phys. Rev. B **97** (2018) 081107(R).

[6] S. Hayami, H. Kusunose, and Y. Motome, Phys. Rev. B **97** (2018) 024414.

[7] Y. Sugita, T. Miyake, and Y. Motome, Phys. Rev. B **97** (2018) 035125 [*selected in Kaleidoscope*].

[8] Y. Sugita, T. Miyake, and Y. Motome, preprint Physica B: Cond. Matter, in press.

[9] R. Takashima, Y. Shiomi, and Y. Motome, preprint (arXiv:1804.03780).

[10] J. Yoshitake, J. Nasu, Y. Kato, and Y. Motome, Phys. Rev. B **96** (2017) 024438.

[11] J. Yoshitake, J. Nasu, and Y. Motome, Phys. Rev. B **96** (2017) 064433.

[12] S.-H. Do, S.-Y. Park, J. Yoshitake, J. Nasu, Y. Motome, Y. S. Kwon, D. T. Adroja, D. J. Voneshen, K. Kim, T.-H. Jang, J.-H. Park, K.-Y. Choi, and S. Ji, Nature Physics, **13** (2017) 1079.

[13] J. Nasu, J. Yoshitake, and Y. Motome, Phys. Rev. Lett. **119** (2017) 127204.

[14] Y. Kasahara, K. Sugii, T. Ohnishi, M. Shimozawa, M. Yamashita, N. Kurita, H. Tanaka, J. Nasu, Y. Motome, T. Shibauchi, and Y. Matsuda, preprint (arXiv:1709.10286), accepted for the publication in Phys. Rev. Lett.

[15] P. A. Mishchenko, Y. Kato, and Y. Motome, Phys. Rev. B **96** (2017) 125124.

[16] Y. Kato, Y. Kamiya, J. Nasu, and Y. Motome, Phys. Rev. B **96** (2017) 174409.

[17] R. Sano, Y. Kato, and Y. Motome, Phys. Rev. B **97** (2018) 014408.

Topological phase reduction and magnetoelectric effect in strongly-correlated electron systems with spin-orbit interaction

Norio KAWAKAMI

Department of Physics, Kyoto University,

Kitashirakawa, Sakyo-ku, Kyoto 606-8502

Spin-orbit interaction provides the possibility to manipulate the spin polarization of a material by applying electric fields as desired for spintronics, as well as the possibility to create an inverted gap in the band structure necessary for topologically nontrivial phases. Although many new phenomena can be expected, the interplay between spin-orbit interaction and the Coulomb interaction in strongly correlated materials is still not well understood.

Electron correlation can change the topological classification of a system. For example, Fidkowski and Kitaev have found that for a one-dimensional topological superconductor of class BDI, electron correlation changes the topological classification from Z to Z_8.

We have studied the topological classification of superconducting phases in a superlattice system composed of $CeCoIn_5$/$YbCoIn_5$ layers. We have found that in the case of quad-layer of $CeCoIn_5$ the strongly correlated system is topologically trivial, while eight pairs of helical edge modes are predicted at the non-interacting level. Thus, this system can serve as a test bed for the reduction of the topological classification. [1]

Also, we aimed at understanding the effect of the interplay between the spin-orbit interaction and electron correlation on anomalous transport such as the magnetoelectric effect. We have studied a periodic Anderson model including the Rashba spin-orbit interaction, which describes noncentrosymmetric f-electron materials such as $CePt_3Si$, using the combination of dynamical mean field theory and the numerical renormalization group to calculate transport properties with high precision. Our calculations demonstrate that while at low temperatures the magnetoelectric effect is small due to cancellation effects of bands with different spin polarization, at high temperatures, where f-electrons become localized due to strong interactions, the magnetoelectric effect is strongly enhanced. [2]

References

[1] Tsuneya Yoshida, Akito Daido, Youichi Yanase, and Norio Kawakami: Phys. Rev. Lett. **118** (2017), 147001.

[2] Robert Peters and Youichi Yanase, Phys. Rev. B **97** (2018), 115128.

Microscopic analysis of the vortex state in superconductors using the augmented quasiclassical equations with the Lorentz force, Kopnin force and slope in the density of state

Takafumi KITA
Department of Physics, Hokkaido University
Sapporo, Hokkaido 060-0810

We derived augmented Eilenberger equations that incorporate the following missing force terms: (i) the Lorentz force, (ii) the pair-potential gradient (PPG) force (or Kopnin force), and (iii) the pressure difference arising from the slope in the density of states (DOS). Using it, we studied the vortex-core charging due to the three force terms. This study have been performed to calculate the sign change of the flux-flow Hall coefficient microscopically. We required much memory due to the presences of the spatial inhomogeneity in the system.

The *vortex-core charging* in type-II superconductors has been pointed out to be related to the sign change of the flux-flow Hall conductivity [1], and numerous studies on the charging of a superconducting vortex have been carried out. However, the forces responsible for the charging of a superconducting vortex are not fully understood. This is because all the force terms used to describe charging in superconductors are missing from the standard Eilenberger equations (i.e., the quasiclassical equations of superconductivity) used to study superconductors in a magnetic field microscopically.

The existence of the Lorentz force acting on the supercurrent was first pointed out by London [2]. In 2001, the Lorentz force was microscopically recovered in augmented quasiclassical equations of superconductivity in the Keldysh formalism. The PPG force was first discussed by Kopnin [3]. In recent years, Arahata and Kato first included the Lorentz and PPG force terms in their augmented quasiclassical equations as an extension of the standard quasiclassical equations of superconductivity in the Keldysh formalism [6]. The charging mechanism of a superconducting vortex due to the pressure or chemical potential difference between the normal and superconducting states was first proposed by Khomskii and Freimuth [4]. They regarded the core as a normal region and considered its chemical potential difference from the surroundings due to the particle–hole asymmetry in the DOS. For the general case of the DOS, Khomskii and Kusmartsev have also given a formula for the chemical potential difference between the normal and superconducting states due to the slope in the DOS [7]. However, despite this, quasiclassical equations considering this pressure dependence have not yet been derived microscopically. Therefore, quasiclassical equations for superconductors still have room for improvement.

We perform numerical calculations for the isolated vortex systems of clean s-wave superconductors with a spherical Fermi surface based on the augmented Eilenberger equations. We assume the spin-singlet pairing

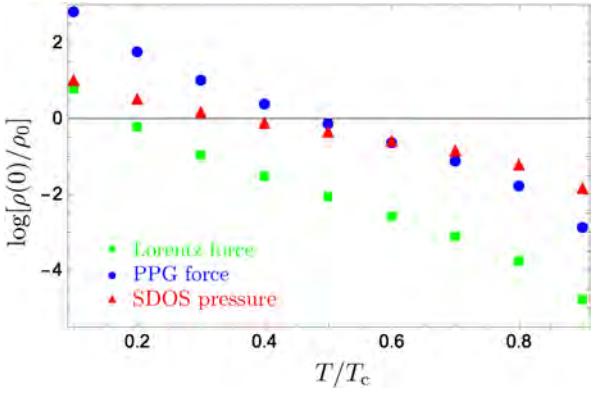

Figure 1: (Color online) Normalized charge density due to the Lorentz force (green square points), PPG force (blue circular points), and SDOS pressure (red triangular points) at the vortex center for $\lambda_0 = 5\xi_0$ as a function of temperature.

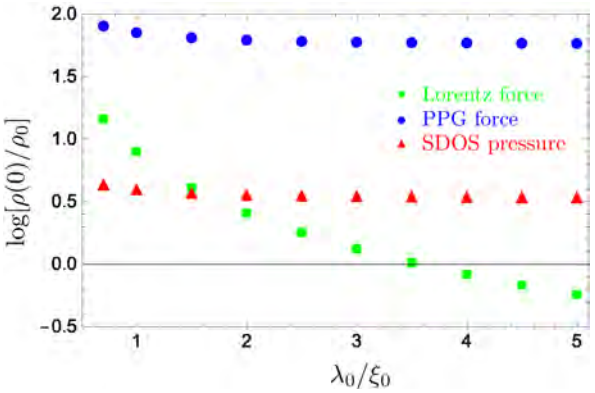

Figure 2: (Color online) Normalized charge density due to the Lorentz force (green square points), PPG force (blue circular points), and SDOS pressure (red triangular points) at the vortex center for $\lambda_0 = 5\xi_0$ as a function of λ_0 calculated for $T = 0.2T_c$.

without spin paramagnetism. The parameters of this system are the coherence length ξ_0, magnetic penetration depth λ_0, Thomas–Fermi screening length λ_{TF}, quasiclassical parameter δ, and the smearing factor η in the advanced and retarded Green functions. We fixed the parameters to $\lambda_{TF} = 0.01\xi_0$, $\delta = 0.01$, and $\eta = 0.01\Delta_0$. Figures 1 and 2 plot the logarithm of the charge density at the vortex center for $\lambda_0 = 5\xi_0$ as a function of temperature and for $T = 0.2T_c$ as a function of λ_0.

We observe that when the London penetration depth is much larger than the coherence length, the contribution of the Lorentz force to the vortex-core charge is negligibly small compared with that of the other forces, the contribution of the SDOS pressure becomes dominant near the transition temperature, and the contribution of the PPG force is so large that the other forces are negligible near absolute zero temperature. We also find that when the London penetration depth is about the same as the coherence length, the contribution of the Lorentz force to the core charge becomes substantial over the value of that of the SDOS pressure, but smaller than that of the PPG force. Thus, because the force that dominantly contributes to quantities may vary with the parameters of the materials, the temperature, the external field, and the system, we need to consider all three forces to study charging and transport phenomena such as the flux-flow Hall effect in type-II superconductors.

References

[1] S. J. Hagen, C. J. Lobb, R. L. Greene, M. G. Forrester, and J. H. Kang, Phys. Rev. B **41**, 11630 (1990).

[2] F. London, *Superfluids* (Dover, New York, 1961), Vol. 1, p. 56.

[3] N. B. Kopnin, J. Low Temp. Phys. **97**, 157 (1994).

[4] D. I. Khomskii and A. Freimuth, Phys. Rev. Lett. **75**, 1384 (1995).

[5] T. Kita, Phys. Rev. B **64**, 054503 (2001).

[6] E. Arahata and Y. Kato, J. Low. Temp. Phys. **175**, 364 (2014).

[7] D. I. Khomskii and F. V. Kusmartsev, Phys. Rev. B **46**,14245 (1992).

Microscopic analysis of cuprate superconductors in FLEX-S approximation

Takafumi KITA
Department of Physics, Hokkaido University
Sapporo, Hokkaido 060-0810

Fluctuation-exchange (FLEX) approximation [1] is a method that succeeds in describing various normal-state properties of high-T_c superconductors qualitatively [2]. In the FLEX approximation, we include the contributions of spin fluctuations caused by the Coulomb interaction into the self-energy. We can incorporate not only Feynman diagrams called "ring diagrams" which represent particle-hole scattering processes, but also those called "ladder diagrams" which represent particle-particle scattering processes in this framework.

Subsequently, Dahm and Tewordt performed a theoretical study on the superconducting phase of high-T_c's by incorporating only the particle-hole scattering processes [3]. Specifically, they incorporated some anomalous diagrams characteristic of the superconducting state besides the ring diagrams in the normal state. Their results agree with the properties of the cuprate superconductors which are measured in experiments qualitatively.

FLEX-S approximation [4] adopted in our study is an extension of the FLEX approximation. However, in this improved framework, we can consider both the normal-state and anomalous diagrams systematically beyond the ring and/or ladder approximations by introducing a symmetrized vertex. Therefore, we can incorporate more processes from spin fluctuations than the previous framework.

In our study, we calculated one particle Green's function for cuprate superconductors using both frameworks, i.e., Dahm-Tewordt framework and FLEX-S approximation. We compared the density-of-states between the two frameworks that can be obtained from the one particle Green's function. In both frameworks, we have to solve self-consistently the Dyson–Gor'kov equation and equation for the self-energy given in terms of the one-particle Green's function, and it took a lot of computational cost to perform these calculation. For this reason, we use parallel machine to perform these calculations, so we need to use the supercomputer in ISSP. In our calculation, we use two-dimensional Hubbard model, and the band dispersion $\epsilon_{\mathbf{k}}$ is given as follows

$$\epsilon_{\mathbf{k}} = -2t_0(\cos k_x + \cos k_y) + 4t_1 \cos k_x \cos k_y + 2t_2(\cos 2k_x + \cos 2k_y).$$

t_0, t_1, and t_2 are the first, second, and third nearest neighbor hopping pareameter, and we choose $t_0 = 1, t_1 = 1/6$, and $t_2 = -1/5$ to represent the band structure of YBCO [5]. Moreover, we choose the on-site interaction parameter as $U = 6.5t_0$.

Figure 1 shows the density-of-states in the superconducting state calculated in both frameworks. In this figure, we present the result for dimensionless temperature $T/t_0 = 0.01$ and filling $n = 0.85$. The peak-to-peak values of both lines that represents the value of superconducting pair potential is 0.1 correspond to 10[meV], and it is consistent with the result from STM experiments [6]. However, we can't find a large difference between two lines in Fig.

1.

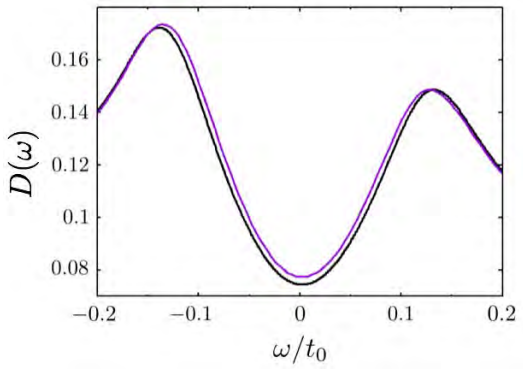

Figure 1: The black line is calculated by the FLEX-S approximation, and purple one is calculated in the framework that incorporates particle-hole scattering processes.

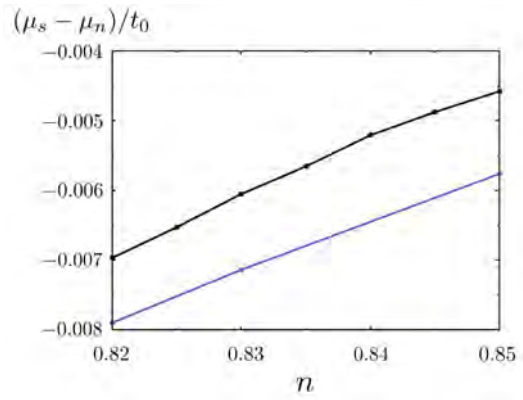

Figure 2: The black line is calculated in the FLEX-S approximation, and purple one is calculated in the framework that incorporates particle-hole scattering processes.

Figure 2 compares the chemical-potential difference between the normal and superconducting states calculated in the two frameworks using the same parameters at $T/t_0 = 0.01$. We can see that the difference between two results is about 10% at most. So we conclude that the ladder diagrams contribute little to the physical property obtained from one particle Green's function in this model.

This framework is important to obtain the precise temperature and filling dependence of various physical properties in the superconducting state concisely. We are planning to investigate the difference between these two frameworks to analyze two particle Green's function or calculate in other models such as the *d*-*p* model. From these, we aim to clalrify various parameter dependences such as the temperature and filling ones more precisely, and we aim to find those physical properties which are overlooked in the previous work where the ladder diagrams were neglected.

References

[1] N. E. Bickers and D. J. Scalapino, Ann. Phys. (N.Y.) **193**, 206 (1989).

[2] H. Kontani, K. Kanki, and K. Ueda, Phys. Rev. B **59**, 15723 (1999).

[3] T. Dahm and L. Tewordt, Phys. Rev. Lett. **74**, 793 (1995).

[4] T. Kita, J. Phys. Soc. Jpn. **80**, 124704 (2011).

[5] T. Tanamoto, H. Kohno, and H. Fukuyama, J. Phys. Soc. Jpn. **61**, 1886 (1992).

[6] Ø. Fischer, M. Kugler, I. M. Aprile, C. Berthod, and C. Renner, Rev. Mod. Phys. **79**, 353 (2007).

Effect of Hund's coupling on non-local correlations in two-orbital Hubbard model

Yusuke Nomura

Department of Applied Physics

The University of Tokyo, Hongo 7-3-1, Bunkyo-ku, Tokyo 113-8656

In multi-orbital strongly correlated materials, it has been found that the Hund's coupling plays a crucial role in the electronic correlations [1]. The Hund's coupling has two effects. It influences the energy scale of the Mott gap, extending the metallic region when the filling is away from half-filling. At the same time, it suppresses the coherence temperature to form the fermi liquid. With these effects, there emerge strongly-correlated metals even when the system is away from Mott insulator. Such kind of strongly-correlated metals are called "Hund's metal".

So far, the effect of Hund's coupling in Hund's metal has mainly been studied by the dynamical mean-field theory (DMFT) [2]. However, the DMFT cannot capture the spatial correlations. Therefore, the effect of Hund's coupling on non-local correlations is still not understood well. In this study, we employ a cluster extension of DMFT [3], cellular DMFT, to study the interplay between Hund's coupling and spatial correlations.

For this purpose, we employ an improved continuous-time quantum Monte Carlo solver based on interaction expansion (CT-INT) [4]. The improved CT-INT makes use of efficient update schemes, "submatrix update" and "double-vertex update". With the improvements, applications to multi-orbital cluster DMFT become feasible [5]. We study the two-orbital Hubbard model on the square lattice using the 2x2 cluster. We set the size of Hund's coupling J_H to be $J_H/U = 1/4$ with U begin the Hubbard interaction.

We first try the model with Ising-type interaction form, namely we neglect spin-flip and pair-hopping interactions. When the filling n is $n = 1.5$ ($n = 2$: half-filled), around $U/t = 16$ ($J_H/t = 4$), we have found that the non-local correlations become significant. If we set $J_H = 0$, we do not see such significant non-local correlations. Therefore, the significant non-local correlations are induced by Hund's coupling. This result suggests that the Hund's coupling strongly affects not only the onsite correlations but also the spatial correlations. The simulations with $SU(2)$ symmetric interactions are now under way.

References

[1] A. Georges, L. de' Medici, and J. Mravlje,

Annual Review of Condensed Matter Physics, **4**, 137 (2013)

[2] A. Georges, G. Kotliar, W. Krauth, and M. J. Rozenberg, Rev. Mod. Phys. **68**, 13 (1996)

[3] T. Maier, M. Jarrell, T. Pruschke, and M. H. Hettler, Rev. Mod. Phys. **77**, 1027 (2005)

[4] Y. Nomura, S. Sakai, and R. Arita, Phys. Rev. B **89**, 195146 (2014)

[5] Y. Nomura, S. Sakai, and R. Arita, Phys. Rev. B **91**, 235107 (2015)

Exotic phenomena induced by topology and strong correlations

Tsuneya YOSHIDA

Department of Physics, Kyoto University,

Kitashirakawa, Sakyo-ku, Kyoto 606-8502

In these years, topological perspective on condensed matter has increased its importance. One of the significant issues of this field is to understand the correlation effects on topological insulators/superconductors where novel phenomena are expected due to combination of these two effects. In particular, it is found that electrons correlations induce the reduction of topological classifications; only eight topologically distinct phases are allowed under the electron correlations for one-dimensional topological superconductors of symmetry class BDI, while infinite number of topologically distinct phases are allowed in the absence of correlations.

This remarkable phenomenon induced by electron correlations is extensively studied in these several years. In spite of the extensive studies, the reduction has not been well understood. In particular, the following questions remain unsolved: (i) what happens in the bulk when the reduction occurs for edges?; (ii) In which systems can one observe the reduction in experiments? In this project, we have addressed these questions.

Firstly, in order to understand bulk behaviors, we have carried out numerical simulation of the reduction phenomena for a weak-topological insulator in two dimensions. Our analysis based on real-space dynamical mean-field theory combined with continuous-time quantum Monte Carlo have elucidated that all of the gapless edge modes are gapped out without symmetry breaking while the bulk remains a band insulator characterized with the winding number w=4. This result indicates that a gapped Mott insulator emerges only around the boundary.

Secondly, we have addressed theoretical proposal of candidate materials of the reduction. Specifically, we have pointed out that the superlattice systems composed of CeCoIn5/YbCoIn5 can be a promising platform for the reduction of topological classification, ZxZ to ZxZ_8; the all of the gapless edge modes are gapped out without symmetry breaking when the number of Ce-layer is multiple of four.

References

[1] Tsuneya Yoshida, Norio Kawakami: Phys. Rev. B **95** (2017), 045127.

[2] Tsuneya Yoshida, Akito Daido, Youichi Yanase, and Norio Kawakami: Phys. Rev. Lett. **118** (2017), 147001.

Numerical Studies on the Superconductivity in Systems with Coexisting Wide and Narrow Bands

KAZUHIKO KUROKI
Department of Physics, Osaka University
1-1 Machikaneyama, Toyonaka, Osaka, 560-0043, Japan

In this report, we present two of the studies, related to superconductivity due to electron correlation, performed in our group in 2017 fiscal year using the supercomputer at ISSP.

HIGH T_c SUPERCONDUCTIVITY ARISING FROM WIDE AND INCIPIENT NARROW BANDS

An ideal situation for realizing high-T_c superconductivity is to have strong pairing interaction and light electron mass simultaneously, but strong pairing interaction usually induces heavy effective mass. In ref.[1], we proposed that high-T_c superconductivity is possible in Hubbard-type systems (with the on-site U) having wide and narrow bands, where light effective mass and strong pairing interaction is realized when the Fermi level sits in the vicinity of, but does not intersect, the narrow band (i.e., the incipient narrow band) (Fig.1). The two-leg Hubbard ladder with diagonal hoppings, a model for the ladder-type cuprates, was studied as a system in which such a situation is realized, where a possible occurrence of extremely high T_c was suggested. More recently, the so-called diamond chain model, which has a flat band and two dispersive bands when a certain condition is satified, was studied using DMRG, and there it was shown that superconductivity is strongly enhanced when the Fermi level sits in the vicinity of, but not within the flat band[2]. Motivated by the study

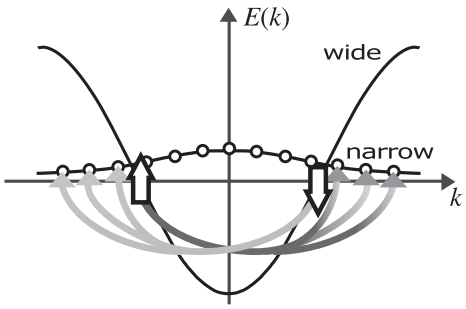

FIG. 1. Schematic image of pair scattering processes in systems with wide and incipient narrow bands

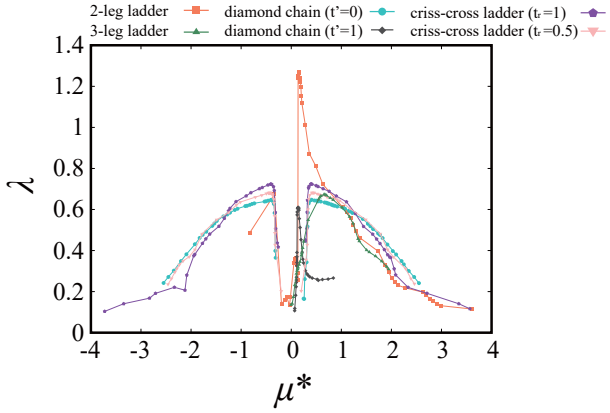

FIG. 2. Eigenvalue of the Eliashberg equation for various systems with wide and flat bands. They are plotted as functions of the chemical potential measured from the flat band energy. The on-site U is taken as $U = 6t$, and the temperature is fixed at $0.05t$, where t is the nearest neighbor hopping.

in ref.[2], in 2017 fiscal year, we have extended the study of ref[1], showing that this high-T_c mechanism works in a variety of systems that consist of wide and incipient narrow (or flat) bands, such as the diamond lattice, three-leg ladder, and the crisscross ladder. We have applied the fluctuation exchange approximation to the Hubbard model on these lattices, and have shown that superconductivity is strongly enhanced when the Fermi level sits close to the narrow band[3](Fig.2). This shows the generality of the mechanism of high-Tc superconductivity originating from wide and incipient narrow bands.

WIDE AND INCIPIENT NARROW BANDS IN RUDDLESDEN-POPPER BILAYER COMPOUNDS ORIGINATING FROM "HIDDEN LADDERS"

In reality, it is very difficult to control carrier doping in ladder-type cuprates. As a way to realize in actual materials the coexising wide and incipient narrow band systems mentioned in the previous section, we have introduced a concept of " hidden ladder " electronic structure in the bilayer Ruddlesden-Popper compounds, where anisotropic d-orbitals give rise to ladder-like elec-

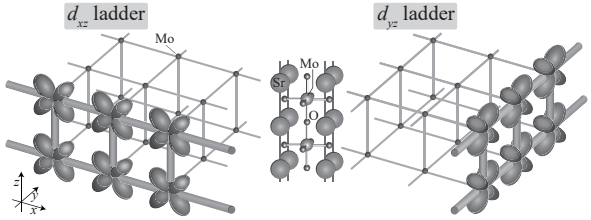

FIG. 3. Schematic image of the hidden ladders in RP327 bilayer systems.

tronic structures[4](Fig.3). Namely, considering the case in which t_{2g} orbitals form the bands crossing (or lie near) the Fermi level, an electron in the $d_{xz/yz}$ orbital selectively hops in the x/y direction as well as in the z direction normal to the bilayer. This means that the $d_{xz/yz}$ orbitals form ladders with x/y and z directions being the leg and rung directions, respectively. Furthermore, considering that the best situation for superconductivity in the ladder-type cuprates occurs for about 30 percent electron doping from half-filling[1], we expect that materials with two electrons per three t_{2g} orbitals (d^2 configuration) should bring about the ideal situation, where the Fermi level sits in the vicinity of the narrow-band edge without large amount of carrier doping. Hence we expect that $Sr_3Mo_2O_7$ and $Sr_3Cr_2O_7$ are good candidates, and this is indeed confirmed from first principles band calculation. We have performed fluctuation exchange study on a 6 orbital model that is derived from the first principles band structure, and proposed the possibility of high-T_c superconductivity in these materials.

[1] K. Kuroki, T. Higashida, and R. Arita, Phys. Rev. B **72**, 212509 (2005).
[2] K. Kobayashi *et al.*, Phys. Rev. B **94**, 214501 (2016).
[3] K. Matsumoto, D. Ogura, and K. Kuroki, Phys. Rev. B **97**, 014516 (2018).
[4] D. Ogura, H. Aoki, and K. Kuroki, Phys. Rev. B **96**, 184513 (2017).

Two-channel Kondo effect and multipole susceptibility

Takashi HOTTA
Department of Physics, Tokyo Metropolitan University
1-1 Minami-Osawa, Hachioji, Tokyo 192-0397

In this research, we have analyzed a seven-orbital impurity Anderson model hybridized with Γ_8 conduction electrons for the case with three local f electrons corresponding to a Nd^{3+} ion by employing a numerical renormalization group technique [1, 2]. The model Hamiltonian is given by

$$H = \sum_{\mathbf{k},\mu,\tau} \varepsilon_{\mathbf{k}} c^{\dagger}_{\mathbf{k}\mu\tau} c_{\mathbf{k}\mu\tau} + \sum_{\mathbf{k},\mu,\tau} V(c^{\dagger}_{\mathbf{k}\mu\tau} f_{a\mu\tau} + \mathrm{h.c.}) + H_{\mathrm{loc}}, \quad (1)$$

where $\varepsilon_{\mathbf{k}}$ is the dispersion of a Γ_8 conduction electron with wave vector $\mathbf{k}$, $c_{\mathbf{k}\mu\tau}$ denotes the annihilation operator of a Γ_8 conduction electron, μ distinguishes the cubic irreducible representation, Γ_8 states are distinguished by $\mu = \alpha$ and β, while Γ_7 and Γ_6 states are labeled by $\mu = \gamma$ and δ, respectively, τ is the pseudo-spin which distinguishes the degeneracy concerning the time-reversal symmetry, $f_{j\mu\tau}$ indicates the annihilation operator of a localized f electron in the bases of (j, μ, τ), j is the total angular momentum, $j = 5/2$ and $7/2$ are denoted by "a" and "b", respectively, V is the hybridization between conduction and localized electrons, and H_{loc} denotes the local f-electron term. In the present case, we consider the hybridization between Γ_8 conduction electrons and the Γ_8 quartet of $j = 5/2$.

The local term, H_{loc}, is given by

$$H_{\mathrm{loc}} = \sum_{j,\mu,\tau} (\lambda_j + B_{j,\mu} + E_f) f^{\dagger}_{j\mu\tau} f_{j\mu\tau} + \sum_{j_1 \sim j_4} \sum_{\mu_1 \sim \mu_4} \sum_{\tau_1 \sim \tau_4} I^{j_1 j_2, j_3 j_4}_{\mu_1\tau_1\mu_2\tau_2,\mu_3\tau_3\mu_4\tau_4} \times f^{\dagger}_{j_1\mu_1\tau_1} f^{\dagger}_{j_2\mu_2\tau_2} f_{j_3\mu_3\tau_3} f_{j_4\mu_4\tau_4}, \quad (2)$$

where $\lambda_a = -2\lambda$, $\lambda_b = (3/2)\lambda$, λ is the spin-orbit coupling of f electron, $B_{j,\mu}$ denotes the CEF potential energy, E_f indicate the f-electron level, and I denotes the Coulomb interactions between f electrons.

The Coulomb interaction I is expressed with the use of four Slater-Condon parameters, F^0, F^2, F^4, and F^6. Although the Slater-Condon parameters of a material should be determined from experimental results, here we simply set the ratio as $F^0/10 = F^2/5 = F^4/3 = F^6 = U$, where U is the Hund rule interaction among f orbitals. The CEF potentials for f electrons from ligand ions are given in the table of Hutchings for the angular momentum $\ell = 3$. For a cubic structure with O_{h} symmetry, CEF parameters are expressed by two CEF parameters, B^0_4 and B^0_6. Following the traditional notation, we define B^0_4 and B^0_6 as $B^0_4 = Wx/F(4)$ and $B^0_6 = W(1-|x|)/F(6)$, respectively, where x specifies the CEF scheme for the O_{h} point group, while W determines the energy scale for the CEF potential. We choose $F(4) = 15$ and $F(6) = 180$ for $\ell = 3$.

Now, we consider the case of $n = 3$ by appropriately adjusting the value of E_f. As U denotes the magnitude of the Hund rule interaction among f orbitals, it is reasonable to set $U = 1$ eV. The magnitude of λ varies between 0.077 and 0.36 eV depending on the type of lanthanide ions. For a Nd^{3+} ion, λ is $870 - 885$ cm^{-1}. Thus, we set $\lambda = 0.11$ eV. Finally, the magnitude of W is typically of the order of millielectronvolts, although it depends on the

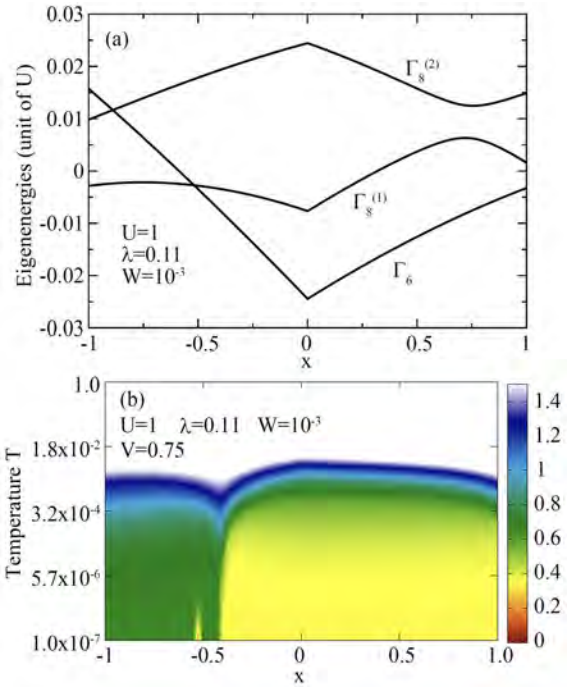

Figure 1: (a) Low-lying eigenenergies of $H_{\rm loc}$ versus x for $n = 3$. (b) Contour color map of the entropy on (x, T) plane for $W = 10^{-3}$.

material. Here, we simply set $|W| = 10^{-3}$ eV.

In Fig. 1(a), we depict curves of ten low-lying eigenenergies of $H_{\rm loc}$ for $n = 3$ since the ground-state multiplet for $W = 0$ is characterized by $J = 9/2$, where J denotes the total angular momentum of multi-f-electron state. We appropriately shift the origin of the energy to show all the curves in the present energy range. We emphasize that the results are almost the same as those of the LS coupling scheme. For the case of $W > 0$, we find the $\Gamma_8^{(1)}$ ground state for $x \leq -0.5$, while the Γ_6 ground state is observed for $x \geq -0.5$. However, for $W < 0$, the Γ_6 ground state appears only in the vicinity of $x = -1.0$. For the wide range of $-0.9 < x \leq 1$, we obtain another $\Gamma_8^{(2)}$ ground state.

In this study, we analyze the model by employing a numerical renormalization group (NRG) method. We introduce a cut-off Λ for the logarithmic discretization of the conduction band. Owing to the limitation of computer resources, we keep M low-energy states. Here, we use $\Lambda = 5$ and $M = 4,000$. In the following calculations, the energy unit is D, which is a half of the conduction band width. Namely, we set $D = U = 1$ eV in this calculation. In the NRG calculation, the temperature T is defined as $T = \Lambda^{-(N-1)/2}$ in the present energy unit, where N is the number of renormalization steps.

In Fig. 1(b), we show the contour color map of the entropy for $W = 10^{-3}$ and $V = 0.75$. To visualize precisely the behavior of entropy, we define the color of the entropy between 0 and 1.5, as shown in the right color bar. We immediately notice that an entropy of $\log 2$ (green region) appears at low temperatures for $-1.0 < x < -0.4$, while an entropy of $0.5 \log 2$ (yellow region) is found for $-0.4 < x < 1.0$. The region with an entropy of $0.5 \log 2$ almost corresponds to that of the Γ_6 ground state in comparison with Fig. 1, although we find a small difference between them around $x \sim 0.5$. The residual entropies, $0.5 \log 2$ and $\log 2$, are eventually released at extremely low temperatures in the numerical calculations. Approximately at $x = -0.5$, the release of an entropy of $\log 2$ seems to occur at relatively high temperatures. This is considered to be related with the accidental degeneracy of Γ_6 and $\Gamma_8^{(1)}$ states. In any case, the details on the entropy behavior at low temperatures will be discussed elsewhere in the future.

In summary, we have found the two-channel Kondo effect in the seven-orbital impurity Anderson model hybridized with Γ_8 conduction electrons for the case of $n = 3$ with the local Γ_6 ground state. In near future, we expect that the two-channel Kondo effect will be discovered in Nd 1-2-20 compounds.

References

[1] T. Hotta, J. Phys. Soc. Jpn. **86**, 083704 (2017).

[2] T. Hotta, Physica B **536C**, 203-210 (2018).

Numerical study on interplay between stripes and electron-phonon interactions in the Hubbard model

Takahiro OHGOE

Department of Applied Physics, The University of Tokyo,

7-3-1 Hongo, Bunkyo-ku, Tokyo 113-0033

Since the discovery of high- T_c cuprates, many experiments have been performed to unveil its mechanism and revealed its rich and complex physics. Especially in the underdoped region, exotic phenomena such as pseudogap or stripe order were observed and they are still intensively studied both experimentally and theoretically. Owing to the recent advancements of the scanning tunneling microscope (STM) and X-ray experiments, charge orders have been widely observed in the underdoped region of several families of high-T_c cuprates, establishing their presence as a universal feature [1].

In our recent work [2], we studied the stripe states in the Hubbard model by using the many-variable variational Monte Carlo (mVMC) method. As a result, we found that several stripes with different periodicities are severely competing especially in the underdoped region. Furthermore, we found that the ground states are stripe states instead of homogeneous superconducting state for the doping concentration $0.1 \lesssim \delta \lesssim 0.3$. However, the electron-phonon interactions are neglected and its roles on stripes remains elusive.

In this study, we studied the effect of electron-phonon interactions on the competition between stripe states and homogeneous states. To this purpose, we used the extended VMC method for electron-phonon coupled systems which we proposed [3]. As a result, we found that electron-phonon interactions with realistic phonon frequencies do not change the physical quantities such as spin/charge structure factors so much. On the other hand, it has been turned out that the electron-phonon interactions can change the ground states from stripe states to homogeneous states. In this study, we considered the particular modes of phonons individually. The more realistic analysis based on fully ab-initio electron-phonon interactions will be reported elsewhere.

References

[1] R. Comin and A. Damascelli, Annu. Rev. Condens. Matter Phys. **7**, 369 (2016)

[2] K. Ido, T. Ohgoe and M. Imada, Phys. Rev. B. **97**, 045138 (2018)

[3] T. Ohgoe and M. Imada, Phys. Rev. B **89**, 195139(2014)

Quantum Monte Carlo approach to local electronic correlations in unconventional superconductors

Shintaro HOSHINO
Department of Physics, Saitama University, Saitama 338-8570, Japan

Unconventional superconductivity in strongly correlated electron systems has been one of the central issues in condensed matter physics due to their rich physical properties and presence in a wide range of materials with p, d, f electrons. Fullerene-based superconductors are typical cases which show unconventional superconductivity, where the Mott insulator phase is located near superconducting phase [1]. Since the symmetry of pairing state is identified as s-wave, the local electronic correlations are capable to describe its physical properties which are still different from that of conventional BCS superconductors. For A_3C_{60}, the three electrons are doped per fullerene molecule. The underlying mechanism for superconductivity has been clarified as an effectively sign-reversed Hund's coupling. With this antiferromagnetic Hund coupling, the low-spin state is favored instead of high-spin state for usual Hund's rule coupling. Recent experiments show the presence of the anomalous metalic state [2]. Once electrons are localized in the Mott phase, the electron-phonon coupling leads to the defomation of the fullerene molecule, which has been detected by the IR spectroscopy. On the other hand, the metalic regime show a neary spherical shape. Interestingly, in the metallic regime close to the Mott phase, the fulleren molecule is detected to be deformed, which is called the Jahn-Teller metal [2], as distinct from the above two cases.

As a microscopic origin for the Jahn-Teller metal, we have theoretically proposed the spontaneous orbital-selective Mott transition [6] using the dynamical mena-field theory combined with quantum Monte Carlo method (DMFT+CTQMC) [3, 4]. We have further clarified the characteristics of this phase based on the realistic band structures derived in Ref. [5]. It is found that once the system enters into the Jahn-Teller metal phase, the strongly anisotropic conductivity appears [7]. Recently, using the supercomputer in ISSP, the University of Tokyo, the phase diagram for the doping regime has also been mapped out by means of the DMFT+CTQMC. For a strong coupling regime, the orbital order that breaks original cubic symmetry has been found. The superconducting region shrinks by tuning the number of the doped electrons from three toward two per fullerene. At the filling number two, the low-spin Mott insulator is realized. These results would be useful to explore the pressure and carrier number dependences experimentally.

References

[1] Y. Takabayashi et al., Science **323**, 1585 (2009).

[2] R.H. Zadik et al., Sci. Adv. **1**, e1500059 (2015).

[3] P. Werner et al., Phys. Rev. B **74**, 155107 (2006).

[4] E. Gull et al., Rev. Mod. Phys. **83**, 349 (2011).

[5] Y. Nomura, K. Nakamura and R. Arita, Phys. Rev. B **85**, 155452 (2012).

[6] S. Hoshino and P. Werner, Phys. Rev. Lett. **118**, 177002 (2017).

[7] S. Hoshino, R. Arita and P. Werner, talk at JPS March Meeting (2018).

Theoretical study of strong correlations in $Cd_2Os_2O_7$

Hiroshi Shinaoka
Department of Physics, Saitama University, 338-8570, Japan

The pyrochlore oxide $Cd_2Os_2O_7$ is one of the few compounds whose low-T magnetic structure has been experimentally determined among a number of magnetic $5d$ pyrochlore oxides. Os^{5+} ions have a $5d^3$ configuration, where t_{2g} is half-filled. This compound exhibits a magnetic transition at $T \simeq 227$ K accompanied by a change of the temperature dependence of the resistivity from metallic behavior to insulator one [1]. The low-T magnetic structure was identified as the so-called all–in–all–out magnetic oder by resonant X-ray scattering [2]. Then, this was supported by a first-principles study based on local-density-approximation (LDA) + U method [3]. The LDA+U calculations indicate that the metal-insulator transition is a Lifshitz transition driven by the emergence of the magnetic order. However, there has been no finite-T first-principles calculations for the compound. Thus, the origin of the finite-T transition still remain to be solved.

In this project, we performed a finite-T first-principles calculations based on the dynamical mean-field theory (DMFT). We constructed a three-orbital tight-binding model for the t_{2g} manifold projected on the maximally localized Wannier functions. We employed a first-principles code, Quantum ESPRESSO, for constructing the maximally localized Wannier functions in the two-component formalism. In the DMFT calculations, we solved quantum impurity problems by the continuous-time quantum Mote Carlo method using the current state-of-the-art implementation [4].

Figure 1 shows the computed momentum-resolved spectrum function $A(k, \omega)$ at $U = 2$ eV for different temperatures T. The all–in–all–out magnetic order emerges at low T. Below the magnetic transition temperature, the quasi-particle bands are split and the spectrum is gapped out. This is consistent with the scenario of the Lifshitz transition. The quasi-particle bands survive down to the lowest T computed, being in a clear contrast to the Mott nature of the insulating pyrochlore oxides [5].

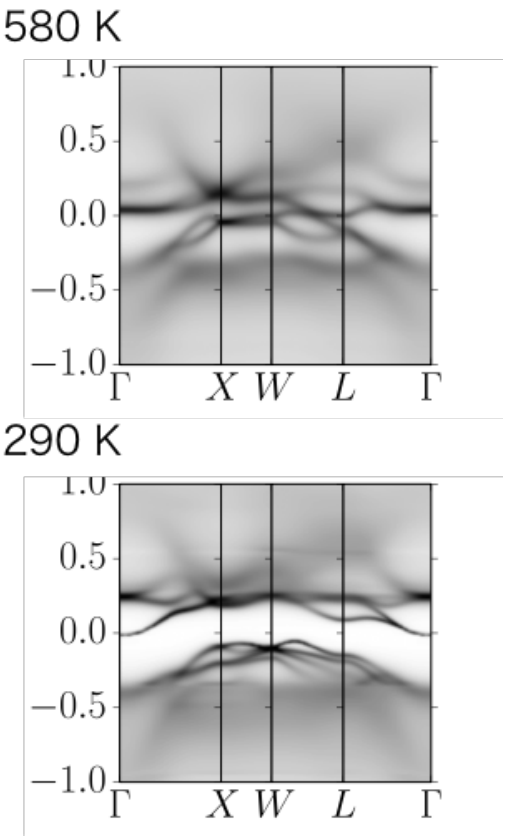

Figure 1: Momentum-resolved spectrum $A(k, \omega)$ computed with $U = 2$ eV.

The above results were obtained in a collaboration with Y. Nomura, T. Kondo and M.

Nakayama.

References

[1] For a review, Z. Hiroi, J. Yamaura, T. Hirose, I. Nagashima, and Y. Okamoto, APL Materials **3**, 041501 (2015).

[2] J. Yamaura *et al.*, Phys. Rev. Lett. **108**, 247205 (2012).

[3] H. Shinaoka, T. Miyake, and S. Ishibashi, Phys. Rev. Lett. **108**, 247204 (2012).

[4] H. Shinaoka, E. Gull, P. Werner, Computer Physics Communications **215**, 128 (2017).

[5] H. Shinaoka, S. Hoshino, M. Troyer, and P. Werner, PRL **115**, 156401 (2015).

Dynamical mean-field calculations of electronic states and multipolar fluctuations in strongly correlated electron systems

Junya OTSUKI
Department of Physics, Tohoku University, Sendai 980-8578

Interesting magnetic properties are often observed in transition-metal and rare-earth compounds. Those includes orbital ordering in $3d$ electron systems and multipolar ordering in $4f$ electron systems. For theoretical descriptions of those peculiar ordered states, strong electronic correlations in the atomic orbitals need to be taken into account. For this reason, the dynamical mean-field theory (DMFT) gives a good starting point in studies of long-range ordering observed in strongly correlated electron materials [1].

Here, we give a brief description of our computation scheme based on the DMFT implemented on top of first-principles calculations. We first perform DFT calculations within LDA/GGA using `WIEN2k` package on a local computer. The Bloch states are projected to Wannier orbitals using `DFTTools` [2] of `TRIQS` library [3]. An effective lattice Hamiltonian is thus defined. Electronic correlations in a specific orbitals ($4f$ orbital in the case with rare-earth materials) are incorporated through a local self-energy $\Sigma(i\omega_n)$ computed in an effective Anderson impurity problem within DMFT. In actual computation, we applied the Hubbard-I approximation in the strong-coupling regime using an exact diagonalization library, `pomerol` [4], and a `triqs`-converter, `pomerol2triqs1.4` [5]. The correlated band structure $A(\boldsymbol{k}, \omega)$ is obtained in the procedure thus above.

To discuss long-range ordering, we compute the static susceptibilities by solving the Bethe-Salpeter (BS) equation. Since the susceptibilities generally have four orbital indices, it is essentially impractical to compute the full orbital dependence in d or f orbitals without special treatment of the vertex part in the BS equation.

We derived a simplified BS equation which is valid in the strong-coupling regime [6]. We analytically demonstrated that the equation gives kinetic exchange interaction in the Hubbard model and the RKKY interaction in the periodic Anderson model. Practically, the equation requires only a partial information of the vertex part, and hence is possible to treat full orbital dependence of susceptibilities in d and f electron systems. This equation provides a practical way to access multipolar ordering in first-principles-based calculations.

References

[1] G. Kotliar *et al.*, Rev. Mod. Phys. **78**, 865 (2006).

[2] M. Aichhorn *et al.*, Comp. Phys. Comm. **204**, 200 (2016).

[3] O. Parcollet *et al.*, Comp. Phys. Comm. **196**, 398 (2015).

[4] A. E. Antipov, I. Krivenko, and S. Iskakov, `http://doi.org/10.5281/zenodo.825870`

[5] `https://github.com/j-otsuki/pomerol2triqs1.4`

[6] J. Otsuki, K. Yoshimi, and H. Shinaoka, in preparation.

Skyrmion crystal phase in itinerant magnets with spin-orbit coupling

Satoru Hayami
Department of Physics, Hokkaido University, Sapporo, 060-0810

Noncoplanar magnetic textures have attracted great interest in condensed matter physics, as they often lead to topologically nontrivial quantum states and related intriguing phenomena. Such noncoplanar magnetic orders have been extensively studied in noncentrosymmetric systems where the spin-orbit coupling plays an essential role. For example, skyrmion crystals with noncoplanar spin textures are stabilized in noncentrosymmetric crystals under an applied magnetic field. These skyrmion crystals are categorized according to their vorticity and helicity: a Bloch-type skyrmion with the helicity $\pm\pi/2$ in chiral magnets with the Dresselhaus-type spin-orbit coupling in Fig. 1(a) and a Néel-type one with the helicity 0 or π in polar magnets with the Rashba-type spin-orbit coupling in Fig. 1(b).

In this project, we investigate how the interplay between the spin-orbit coupling and spin-charge coupling in magnetic conductors affects the formation of noncoplanar magnetic textures [1]. To this end, we begin with a Kondo lattice model with the spin-orbit coupling on a square lattice in polar systems. The Hamiltonian is given by

$$\begin{aligned}\mathcal{H} &= \sum_{\mathbf{k}\sigma}(\varepsilon_{\mathbf{k}}-\mu)c^{\dagger}_{\mathbf{k}\sigma}c_{\mathbf{k}\sigma}+J_{\rm K}\sum_{\mathbf{kq}}\mathbf{s}_{\mathbf{k}+\mathbf{q}}\cdot\mathbf{S}_{\mathbf{q}} \\ &+ \sum_{\mathbf{k}}\mathbf{g}_{\mathbf{k}}\cdot c^{\dagger}_{\mathbf{k}\sigma}\boldsymbol{\sigma}_{\sigma\sigma'}c_{\mathbf{k}\sigma'}, \qquad (1)\end{aligned}$$

where $c^{\dagger}_{\mathbf{k}\sigma}$ ($c_{\mathbf{k}\sigma}$) is a creation (annihilation) operator of an itinerant electron at wave number $\mathbf{k}$ and spin σ. The first term in Eq. (1) represents the kinetic energy of itinerant electrons where $\varepsilon_{\mathbf{k}}$ is the energy dispersion and μ is the chemical potential. The second term represents the spin-charge coupling between itinerant electron spins and localized spins where $\boldsymbol{s}_{\boldsymbol{k}+\boldsymbol{q}}=\sum_{\sigma\sigma'}c^{\dagger}_{\mathbf{k}\sigma}\boldsymbol{\sigma}_{\sigma\sigma'}c_{\mathbf{k}+\mathbf{q}\sigma'}$, $\boldsymbol{\sigma}=(\sigma^x,\sigma^y,\sigma^z)$ is the vector of Pauli matrices, $\mathbf{S}_{\mathbf{q}}$ is the Fourier transform of a localized spin $\mathbf{S}_i$ at site i with the fixed length $|\mathbf{S}_i|=1$, and $J_{\rm K}$ is the exchange coupling constant (the sign of $J_{\rm K}$ is irrelevant owing to the classical spins). The third term in Eq. (1) represents the antisymmetric spin-orbit coupling, which originates from the atomic spin-orbit coupling in noncentrosymmetric systems. In the present model, this term represents the Rashba-type spin-orbit coupling: $\mathbf{g}_{\mathbf{k}}=(g^x_{\mathbf{k}},g^y_{\mathbf{k}})\propto(\sin k_y,-\sin k_x)$, which is induced by the mirror symmetry breaking with respect to the square-lattice plane.

Instead of directly examining the ground state of the model in Eq. (1), we here extract important magnetic contributions by deriving an effective spin model, whose Hamiltonian is summarized as

$$\begin{aligned}\mathcal{H} &= -2\sum_{\eta}\sum_{\alpha\beta}J^{\alpha\beta}_{\eta}S^{\alpha}_{\mathbf{Q}_\eta}S^{\beta}_{-\mathbf{Q}_\eta} \\ &- 2i\sum_{\eta}\mathbf{D}_{\eta}\cdot(\mathbf{S}_{\mathbf{Q}_\eta}\times\mathbf{S}_{-\mathbf{Q}_\eta})-H\sum_i S^z_i, \qquad (2)\end{aligned}$$

where the sum of η is taken for the set of $\mathbf{Q}_\eta$ giving the multiple maxima in the bare susceptibility of itinerant electrons. $J^{\alpha\beta}_{\eta}$ and $\mathbf{D}_{\eta}$ are the coupling constants for symmetric and antisymmetric exchange interactions in momentum space ($\alpha,\beta=x,y,z$), which are long-ranged in real space. These exchange cou-

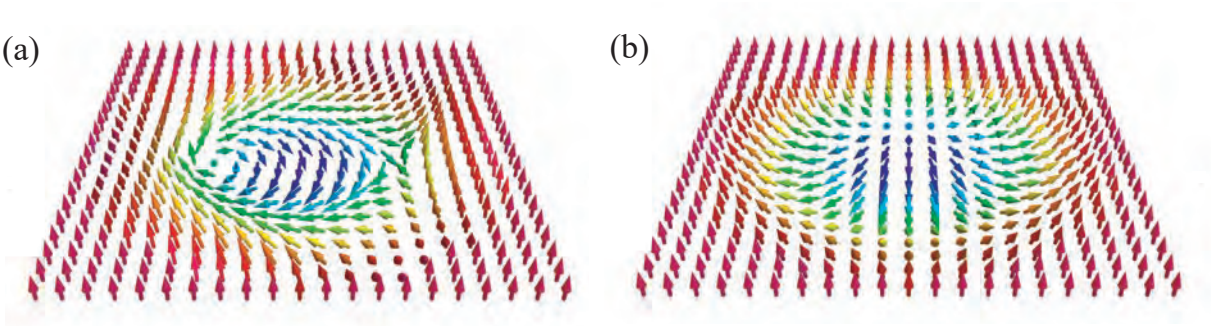

Figure 1: Schematic pictures of (a) Bloch-type and (b) Néel-type spin textures.

plings are related to the second-order perturbative Hamiltonian with respect to $J_{\rm K}$. In Eq. (2), we add the Zeeman coupling to an external magnetic field in the out-of-plane direction. The model in Eq. (2) will give a good approximation under two conditions: (1) $J_{\rm K}$ is small enough compared to the bandwidth of itinerant electrons and (2) the bare susceptibility shows conspicuous peaks at $\mathbf{Q}_\eta$ in the Brillouin zone.

We investigate the magnetic phase diagram of the effective spin model in Eq. (2) by performing simulated annealing from high temperature. Our simulations are carried out with the standard Metropolis local updates under periodic boundary conditions in both directions. In the simulation, we first perform simulated annealing to find the low-energy configuration by gradually reducing the temperature with the rate $T_{n+1} = \alpha T_n$, where T_n is the temperature in the nth step. We set the initial temperature $T_0 = 10^{-1}$-10^{0} and take the coefficient $\alpha = 0.9995$-0.9999. The final temperature, which is typically taken at $T = 10^{-4}$, is reached after 10^5-10^6 Monte Carlo sweeps in total.

As a result, we discover a vortex crystal of Néel type even in the absence of a magnetic field. Furthermore, we demonstrate that a Bloch-type vortex crystal, which is usually associated with the Dresselhaus-type spin-orbit coupling, can also be stabilized in the Rashba-based model. We also show that a magnetic field turns the vortex crystals into Néel- and Bloch-type skyrmion-like crystals with a finite scalar chirality. Our results indicate that a variety of noncoplanar spin textures including vortices and skrymions can be realized and controlled by the interplay between the spin-orbit coupling and the spin-charge coupling in itinerant magnets.

References

[1] S. Hayami and Y. Motome, preprint (arXiv: 1803.01543).

Theoretical studies of strongly correlated electron systems by variational cluster approximation

Atsushi Yamada
Department of Physics, Chiba University
Chiba 263-8522, Japana, Chiba 277-8581

When kinetic and Coulomb repulsion energies are competing, low dimensional materials with geometric frustration exhibit rich phenomena like superconductivity with various pairing symmetries and purely paramagnetic insulator (spin liquid). The organic charge-transfer salts κ-(BEDT-TTF)$_2$X [1, 2, 3, 4] are good examples of such materials, where a transition from paramagnetic metal to spin liquid (Mott transition) has been detected with X=$Cu_2(CN)_3$[3, 4].

We have studied the magnetic and metal-to-insulator transitions of some systems[5, 6, 7] using variational cluster approximation(VCA)[8, 9, 10]. For example, spin liquid state in κ-(BEDT-TTF)$_2$X is analyzed in Ref **??**.

VCA is an extension of the cluster perturbation theory[8] based on the self-energy-functional approach.[10] This approach uses the rigorous variational principle $\delta\Omega_{\mathbf{t}}[\Sigma]/\delta\Sigma = 0$ for the thermodynamic grand-potential $\Omega_{\mathbf{t}}$ written as a functional of the self-energy Σ

$$\Omega_{\mathbf{t}}[\Sigma] = F[\Sigma] + \mathrm{Tr}\ln(-(G_0^{-1} - \Sigma)^{-1}). \quad (1)$$

In the above expression, $F[\Sigma]$ is the Legendre transform of the Luttinger-Ward functional[11] and the index $\mathbf{t}$ denotes the explicit dependence of $\Omega_{\mathbf{t}}$ on all the one-body operators in the Hamiltonian. The stationary condition for $\Omega_{\mathbf{t}}[\Sigma]$ leads to the Dyson's equation. All Hamiltonians with the same interaction part share the same functional form of $F[\Sigma]$, and using that property $F[\Sigma]$ can be evaluated from the exact solution of a simpler Hamiltonian H', though the space of the self-energies where $F[\Sigma]$ is evaluated is now restricted to that of H'. In VCA, one uses for H' a Hamiltonian formed of clusters that are disconnected by removing hopping terms between identical clusters that tile the infinite lattice. Rewriting $F[\Sigma]$ in Eq. 1 in terms of the grand-potential $\Omega' \equiv \Omega'_{\mathbf{t}}[\Sigma]$ and Green function $G'^{-1} \equiv G_0'^{-1} - \Sigma$ of the cluster Hamiltonian H', the grand-potential is expressed as

$$\Omega_{\mathbf{t}}(\mathbf{t}') = \Omega' \int_C \frac{d\omega}{2\pi} \mathrm{e}^{\delta\omega} \sum_{\mathbf{K}} \ln\det\left(1 + (G_0^{-1} - G_0'^{-1})G'\right) \quad (2)$$

and is now a function of $\mathbf{t}'$, which denotes all the one-body operators in H'. The functional trace has become an integral over the diagonal variables (frequency and super-lattice wave vectors) of the logarithm of a determinant over intra-cluster indices. The frequency integral is carried along the imaginary axis and $\delta \to +0$. The stationary solution of $\Omega_{\mathbf{t}}(\mathbf{t}')$ and the exact self-energy of H' at the stationary point, denoted as Σ^*, are the approximate grand-potential and self-energy of H in VCA.

In our analyses we have exactly diaogonalized H' numerically using Lanczos methods. Parts of numerical calculations were done using the computer facilities of the ISSP. We now try to improve our exact diagonalization program using the computer facilities of the ISSP.

References

[1] S. Lefebvre , P. Wzietek, S. Brown, C. Bourbonnais, D. Jérome, C. Mézière, M. Fourmigué, and P. Batail, Phys. Rev. Lett. **85**, 5420 (2000).

[2] Y. Shimizu, K. Miyagawa, K. Kanoda, M. Maesato, and G. Saito, Phys. Rev. Lett. **91**, 107001 (2003).

[3] F. Kagawa, T. Itou, K. Miyagawa, and K. Kanoda, Phys. Rev. B **69**, 064511 (2004).

[4] R.S. Manna, M. de Souza, A. Brühl, J.A. Schlueter, and M. Lang, Phys. Rev. Lett. **104**, 016403 (2010).

[5] A. Yamada, K. Seki, R. Eder, and Y. Ohta, Phys. Rev. B **83**, 195127 (2011); Phys. Rev. B **88**, 075114 (2013).

[6] A. Yamada, Phys. Rev. B **89**, 195108 (2014).

[7] A. Yamada, Phys. Rev. B **90**, 235138 (2014); Phys. Rev. B **90**, 245139 (2014); Int. J. Mod. Phys. B **30**, 1650158 (2016).

[8] D. Sénéchal, D. Perez, and M. Pioro-Ladriére, Phys. Rev. Lett. **84**, 522 (2000); D. Sénéchal, D. Perez, and D. Plouffe, Phys. Rev. B **66**, 075129 (2002).

[9] M. Potthoff, M. Aichhorn, and C. Dahnken, Phys. Rev. Lett. **91** 206402 (2003); C. Dahnken, M. Aichhorn, W. Hanke, E. Arrigoni, and M. Potthoff, Phys. Rev. B **70**, 2451100 (2004).

[10] M. Potthoff, Eur. Phys. J. B **32**, 429 (2003).

[11] L. M. Luttinger and J. C. Ward, Phys. Rev. **118**, 1417 (1960).

Transient dynamics in many electronic systems

Sumio ISHIHARA
Department of Physics, Tohoku University
Aramaki, Aoba, Sendai 980-8578

It is widely recognized that the nonequilibrium steady and transient dynamics in correlated electron systems are one of the central issues in recent modern solid state physics. This research trend is owing to the great development of the experimental techniques as well ans the theoretical calculation methods, for example, the nonequilibrium Green function methods, the numerical real-time dynamics and so on. We report our recent research results obtained by the numerical calculations.

(1) *Non equilibrium light induced dynamics in the double exchange system.* We analyze the light induced dynamics in the double exchange (DE) model [1]. The intense pulse/CW light are applied to the ferromagnetic metallic phase which is widely realized in the DE model. We show by solving numerically the Schrödinger equation and Landau-Lifshitz-Gilbert equation that the DE interaction in highly photoexcited states is antiferromagnetic, an almost perfect Néel state (see Fig. 1). A time characterizing the ferromagnet-to-antiferromagnet conversion is scaled by light amplitude and frequency. This observation is highly in contrast to the conventional DE interaction in the thermal equilibrium state in which the carrier motion promotes the ferromagnetic state. This hidden antiferromagnetic interaction is attributable to the electron-spin coupling under nonequilibrium electron distribution.

(2) *Dynamical localization in Hubbard model.* Suppression of electron motion under an alternating current electric field, termed the dynamical localization effect, is examined in a one-dimensional Hubbard model [2]. It is found by using the iTEBD method that magnitudes of the kinetic-energy suppressions are influenced sensitively by the Coulomb interaction as well as the electron density. The results are interpreted as a combined effect of the Coulomb interaction and the AC field, and provide a guiding principle for the photocontrol of correlated electron motion.

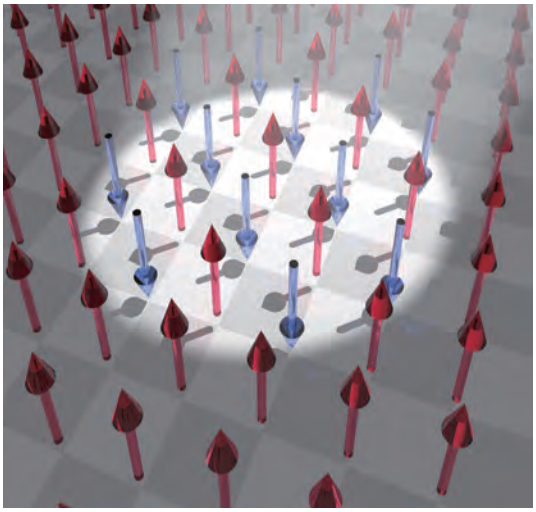

Figure 1: A schematic view of the light induced spin conversion.

References

[1] A. Ono and S. Ishihara: Phys. Rev. Lett. **119** (2017) 207202.

[2] A. Ono, H. Hashimoto, and S. Ishihara: Phys. Rev. B **95** (2017) 085123.

Quantum Monte Carlo simulation and electronic state calculations in correlated electron systems

Takashi YANAGISAWA
Electronics and Photonics Research Institute
National Institute of Advanced Industrial Science and Technology (AIST)
AIST Central 2, 1-1-1 Umezono, Tsukuba 305-8568

We investigated the ground-state properties of strongly correlated electron systems by using an optimization variational Monte Carlo method for two-dimensional Hubbard model. We improved wave functions by taking into account intersite correlations to go beyond the Gutzwiller ansatz. The wave function is an $\exp(-\lambda K)-P_G$-type wave function, which can be improved systematically by multiplying by P_G and $e^{-\lambda K}$ where K is the kinetic-energy operator.

The on-site Coulomb interaction U induces strong antiferromagnetic (AF) correlation. The AF correlation increases as U increases in weakly correlated region. The AF correlation has a peak at U_c, in the intermediate region of U, and decreases as U increases further. U_c is of the order of the bandwidth. This is a crossover from weakly correlated region to strongly correlated region induced by U. We expect that there is a large fluctuation when AF correlation is suppressed. Our idea is that this large fluctuation induces high-temperature superconductivity.

The single-band Hubbard model is given by

$$H = \sum_{ij\sigma} t_{ij} c^{\dagger}_{i\sigma} c_{j\sigma} + U \sum_{i} n_{i\uparrow} n_{i\downarrow}, \qquad (1)$$

where t_{ij} are transfer integrals and U is the on-site Coulomb energy. The transfer integral t_{ij} is non-zero $t_{ij} = -t$ for nearest-neighbor pair $\langle ij \rangle$ and $t_{ij} = -t'$ for next-nearest neighbor $\langle\langle ij \rangle\rangle$. Otherwise t_{ij} vanishes. We denote the number of sites as N and the number of electrons as N_e. The energy unit is given by t.

The well-known Gutzwiller wave function is given by $\psi_G = P_G \psi_0$ where P_G is the Gutzwiller operator defined by $P_G = \prod_j (1-(1-g) n_{j\uparrow} n_{j\downarrow})$ with the variational parameter g in the range of $0 \leq g \leq 1$. The one way to improve the wave function is to take account of nearest-neighbor doublon-holon correlation: $\psi_{d-h} = P_{d-h} P_G \psi_0$. We can take into account inter-site correlations by multiplying by P_J such as $P_J P_{d-h} P_G \psi_0$.

In our study, we take account of inter-site correlation by multiplying the Gutzwiller function by the kinetic operator. A typical wave function of this type is written as[1]

$$\psi_\lambda \equiv \psi^{(2)} = e^{-\lambda K} P_G \psi_0, \qquad (2)$$

where K is the kinetic term in the Hamiltonian: $K = \sum_{ij\sigma} t_{ij} c^{\dagger}_{i\sigma} c_{j\sigma}$ and λ is a variational parameter to be optimized to lower the energy. This wave function is further improved by multiplying $\psi^{(2)}$ by the Gutzwiller operator again: $\psi^{(3)} \equiv P_G \psi_\lambda = P_G e^{-\lambda K} P_G \psi_0$. The expectation values are evaluated by using the variational Monte Carlo method.

The trial wave function $P_{d-h} P_G \psi_0$ was used to develop the physics of Mott transition following the suggestion that the Mott transition occurs due to doublon-holon binding. We examined the Mott transition with the wave function $e^{-\lambda K} P_G \psi_0$[4] because the variational energy by this wave function is much lower than that of the doublon-holon wave function.

The correlation function $S(\mathbf{q})$ has a maximum at $\mathbf{q} = (\pi, \pi)$. $S(\pi, \pi)$ has a peak near $U \simeq 10t$. The spin correlation is suppressed when U is extremely large being larger than the bandwidth. There is a crossover from weakly to strongly correlated regions as U increases. The antiferromagnetic correlation induced by U is reduced for hole doping when U is large. being greater than the bandwidth.

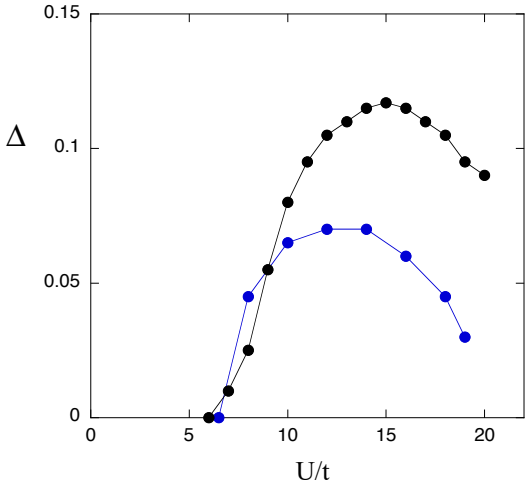

Figure 1: Superconducting order parameter as a function of U in units of t on 10×10 lattice. The number of electrons is $N_e = 88$ and we set $t' = 0.0$. The upper curve is for the BCS-Gutzwiller function and the lower one is for the optimized wave function.

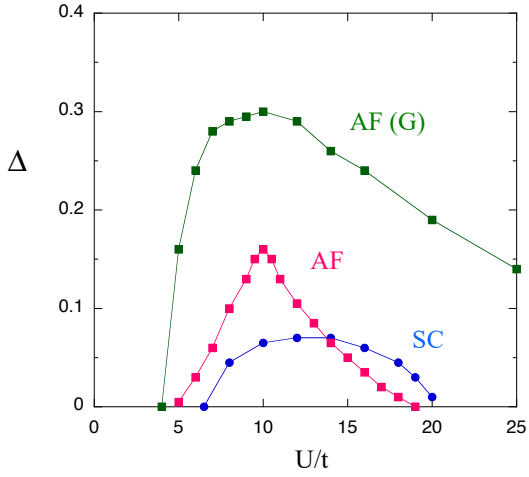

Figure 2: Superconducting and antiferromagnetic order parameters as functions of U in the range of $0 \leq U \leq 25t$ on 10×10 lattice. The number of electrons is $N_e = 88$ and $t' = 0.0$. The solid circles show the SC gap for the improved wave function. The squares represent the antiferromagnetic order parameter, where the upper curve is for the Gutzwiller wave function and the lower curve is for the improved wave function. The boundary condition is periodic in one direction and anti-periodic in the other direction.

The optimized superconducting order parameter Δ increases as U increases, and also has a maximum at some U (Fig.1). We show Δ and the antiferromagnetic (AF) order parameter as functions of U in Fig.2. The superconducting correlation is developed in the region where the AF correlation is suppressed. The reduction of the antiferromagnetic correlation the strongly correlated region suggests the existence of a large antiferromagnetic spin fluctuation. The development of a superconducting correlation is understood to be induced by spin and charge fluctuations that are induced by the process to gain the kinetic energy. The charge fluctuation induced by the kinetic operator is appreciable and helps electrons to form pairs. The spin fluctuation in the strongly correlated region should be distinguished from that in a weakly correlated region. The latter is the conventional spin fluctuation.

The ground-state energy is lowered greatly compared to that of the Gutzwiller wave function. In the strongly correlated region where U is greater than the bandwidth, the AF correlation is reduced, indicating that we have large spin and charge fluctuations. This kind of fluctuations would induce electron pairing and lead to high-temperature superconductivity.

References

[1] T. Yanagisawa et al., J. Phys. Soc. Jpn. 67, 3867 (1998).

[2] T. Yanagisawa, Phys. Rev. B75, 224503 (2007) (arXiv: 0707.1929).

[3] T. Yanagisawa, New J. Phys. 15, 033012 (2013).

[4] T. Yanagisawa and M. Miyazaki, EPL 107, 27004 (2014).

[5] T. Yanagisawa, J. Phys. Soc. Jpn. 85, 114707 (2016).

[6] T. Yanagisawa, M. Miyazaki and K. Yamaji, Int. J. Mod. Phys. B32, 1840023 (2018).

Electron-hole doping asymmetry in κ-type molecular conductor

Hiroshi WATANABE
Waseda Institute for Advanced Study, Waseda University
1-6-1 Nishi Waseda, Shinjuku-ku, Tokyo 169-8050

The family of quasi two-dimensional molecular conductors κ-(BEDT-TTF)$_2$X has been extensively studied as a typical example of strongly correlated electron system. Depending on the monovalent anion X, they show various quantum phases such as antiferromagnetic and spin-liquid dimer-Mott insulators, and superconductivity (SC) [1]. Owing to the similarities in the experimental phase diagrams, κ-(BEDT-TTF)$_2$X system is often compared with high-T_c cuprates, which exhibit Mott metal-insulator transition and SC [2]. Recently, carrier doping in κ-(BEDT-TTF)$_2$X has been realized using electric-double-layer transistor [3], and the direct comparison with cuprates becomes possible. The experimental result shows the electron-hole doping asymmetry, reminiscent of the high-T_c cuprates.

Here, we theoretically study the electron-hole asymmetry in κ-(BEDT-TTF)$_2$X by taking account the intradimer charge degree of freedom. We consider a four-band extended Hubbard model including onsite (U) and intersite Coulomb interactions (V_{ij}) with κ-type geometry with the largest hopping integral t_{b_1} as an energy unit. The ground state properties are studied with the variational Monte Carlo (VMC) method. The Gutzwiller-Jastrow type wave function is used for the VMC trial wave function. The system sizes for calculation are from 288 (4×12×6) to 1152 (4×24×12).

Figure 1 shows the ground-state phase diagram for κ-(BEDT-TTF)$_2$X in a n-U/t_{b_1} space. The largest intersite Coulomb interaction is fixed at V_{b_1}/U=0.5. There appear various competing phases and significant electron-hole asymmetry is observed. The SC phase appears only for electron-doped side and its symmetry is the extended-s+$d_{x^2-y^2}$-wave type [4, 5, 6], which is a different type with cuprates .

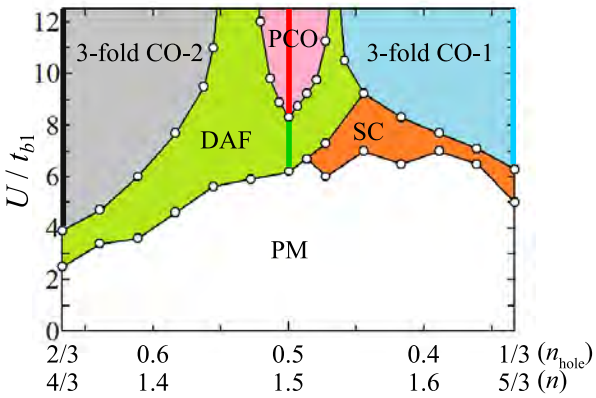

Figure 1: Ground-state phase diagram of the extended Hubbard model for κ-(BEDT-TTF)$_2$X. PM, DAF, PCO, 3-fold CO-1 (2), and SC denote paramagnetic metal, dimer-type antiferromagnetic phase, polar charge-ordered phase, 3-fold charge-ordered phase 1 (2), and superconductivity, respectively.

References

[1] K. Kanoda: J. Phys. Soc. Jpn. **75** (2006) 051007.

[2] R. H. McKenzie: Science **278** (1997) 820.

[3] Y. Kawasugi et al., Nat. Commun. **7** (2016) 12356.

[4] K. Kuroki, T. Kimura, R. Arita, Y. Tanaka, and Y. Matsuda: Phys. Rev. B **65** (2002) 100516(R).

[5] D. Guterding, M. Altmeyer, H. O. Jeschke, and R. Valentí, Phys. Rev. B **94** (2016) 024515.

[6] H. Watanabe, H. Seo, and S. Yunoki: J. Phys. Soc. Jpn. **86** (2017) 033703.